Paper:

Strong Motion Simulation of the M8.0 August 15, 2007, Pisco Earthquake; Effect of a Multi-Frequency Rupture Process

Nelson Pulido[*1], Hernando Tavera[*2], Zenon Aguilar[*3], Shoichi Nakai[*4], and Fumio Yamazaki[*4]

[*1]National Research Institute for Earth Science and Disaster Prevention (NIED)
3-1 Tennodai, Tsukuba, Ibaraki 305-0006, Japan
Email: nelson@bosai.go.jp
[*2]Geophysical Institute of Peru (IGP)
Calle Badajoz # 169, Mayorazgo IV Etapa, Ate Vitarte, Lima, Peru
[*3]Faculty of Civil Engineering, National University of Engineering
Av. Túpac Amaru N° 1150, Lima 25, Peru
[*4]Department of Urban Environment Systems, Chiba University
1-33 Yayoi-cho, Inage-ku, Chiba 263-8522, Japan
[Received November 2, 2012; accepted November 25, 2012]

We investigated the broadband frequency (0.05-30 Hz) radiation characteristics of the August 15, 2007, Mw8.0 Pisco, Peru, earthquake by simulating the near-source strong ground motion recordings in Parcona city (PCN) and Lima city (NNA). A source model of this earthquake obtained from long-period teleseismic waveforms and InSar data shows two separate asperities, which is consistent with the observation of two distinct episodes of strong shaking in strong motion recordings. We constructed a source model that reproduces near-source records at low frequency (0.05-0.8 Hz) as well as high frequency (0.8-30 Hz) bands. Our results show that the aforementioned teleseismic source model is appropriate for simulating near-source low frequency ground motion. Our modeling of the PCN record in the broad-frequency band indicates that a very strong high frequency radiation event likely occurred near the hypocenter, which generated a large acceleration peak within the first episode of strong shaking at PCN. Using this "broadband frequency" source model we simulated the strong ground motion at Pisco city and obtained accelerations as large as 700 cm/s^2 and velocities as high as 90 cm/s, respectively, which may explain the heavy damage occurring in the city.

Keywords: strong motion, source process, Pisco earthquake, Nazca plate, seismic hazard

1. Introduction

The 2007/08/15 (Mw8.0) Peru (Pisco) earthquake was a thrust event originating at the interface of the Nazca and South-American plates slightly north of where the Nazca ridge is being subducted beneath the Peruvian forearc. The source of the Pisco earthquake was located 160 km southeast of Lima off shore from Pisco city in a region filling the gap between the 1974 Mw8.0 Lima earthquake and the 1996 Mw7.7 Nazca ridge earthquake. The earthquake origin time was 23:40:57 UTC, ($-76.51°$E, $-13.35°$N, depth 39 km) [1]. Strong ground motion from this earthquake recorded at Lima city (NNA station) and at a region closer to source area in Parcona city (PCN station) are characterized by two distinct subevents (**Fig. 1**). A visual comparison of these records suggests an atypical ground motion pattern, namely, that the PCN record has a much larger peak acceleration for the first subevent ($\sim$500 gals cm/s^2) than for the second ($\sim$140 cm/s^2) that markedly contrasts with the opposite observation of a peak acceleration larger for the second subevent than for the first at NNA (**Fig. 1**). This feature also holds for velocities observed at PCN and NNA (**Figs. 6b** and **7b**). We investigated the causes of these unusual ground motions by simulating the strong ground motions at these sites. We show that these ground motions are largely influenced by a very complex source process during the Pisco earthquake. Our results suggest that a very strong high frequency radiation episode possibly taking place near the hypocenter may have been responsible for the very large acceleration recorded at PCN (**Fig. 1**).

2. Source Model of the Pisco Earthquake and Observed Strong Ground Motion

The source model of the Pisco earthquake that we use in this study was obtained from a joint inversion of teleseismic body waves and Interferometric Synthetic Aperture Radar data [1]. The model displays two distinct asperities, the first one located near the hypocenter at a depth of 39 km and the second located 60 km south at a depth

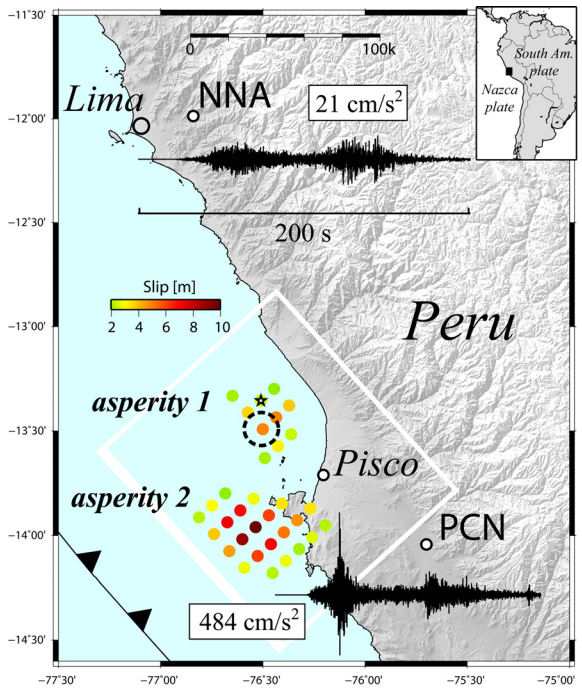

Fig. 1. Strong motion recordings at PCN and NNA stations from the 2007 Mw8.0 Pisco, Peru, earthquake. The map view of the fault plane and slip distribution of the Pisco earthquake used in this study are shown by the white rectangle and color-coded dots. The shallower edge of the fault is indicated by a thicker white line along the strike. Slips smaller than 2 m are not shown. The black dotted region indicates the location of the high frequency radiation event during the earthquake. The star depicts the epicenter of the earthquake.

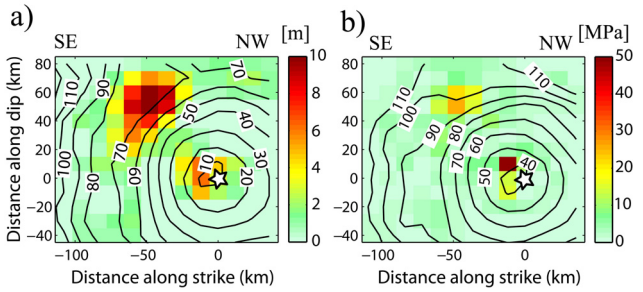

Fig. 2. a) Slip model of the 2007 Mw8.0 Pisco, Peru, earthquake used in this study. Distances within the fault plane refer to the hypocenter (star). Contour lines indicate the propagation of the rupture front each 10 s. b) Stress drop distribution of the earthquake used to simulate BBF strong ground motion records at PCN, NNA and Pisco. Stress drop values were calculated from the slip model in a), except for a subfault near the hypocenter with a large stress drop value, which was set by trial and error to simulate the observed HF strong motions at PCN.

of 17 km (**Figs. 1** and **2a**) with a peak slip of 10 m. The source time function of this earthquake was also characterized by two episodes of moment release corresponding to the aforementioned asperities, the first at 10 s and the second and largest at 60 s [1]. Similar source characteristics have also been obtained by many other slip models of the Pisco earthquake [2–4]. Assuming that these asperities are separated by approximately 65 km, this implies a very low rupture velocity of about 1 km/s (**Fig. 2a**). These features suggest that the earthquake may have been characterized by a delayed rupture of two isolated events, the second being triggered by stress changes induced by the first event [1].

The ground motion recorded at PCN also suggests an anomalous pattern in terms of the source model as the peak acceleration from the first subevent that likely corresponds to the asperity close to the hypocenter (asperity 1), is about 4 times larger than the peak acceleration from the second subevent, which would correspond to the southern asperity (asperity 2), despite the fact that asperity 2 had a much larger moment release [1–4], and is located closer to PCN than asperity 1 (**Fig. 1**). The large difference in peak acceleration between these subevents indicates that they were very unlikely due to site amplifications at PCN. This observation suggests that the source model by Sladen et al. (2010) [1], which was basically obtained from long-period waveforms, as well as Insar data, should be improved or complemented in order to explain the strong high frequency radiation suggested by the very large peak acceleration at PCN.

3. Strong Motion Simulation Method and Source Parameters

To simulate strong motion, we followed the hybrid method of Pulido and Kubo (2004) [5]. This procedure combines the deterministic simulation of ground motion at low frequencies (LF) (0.05-0.8 Hz) with semistochastic simulation at high frequencies (HF) (0.8-30 Hz) to obtain broadband frequency (BBF) (0.05-30 Hz) ground motion. We assume a finite source embedded in a flat-layered 1D velocity structure. In Pulido and Kubo (2004) [5], the source model was defined as a patchwork of rectangles typifying asperities (large slip regions) embedded in a finite fault with a smaller constant slip. In this paper, we improved Pulido and Kubo (2004) [5] simulation to handle the general distribution of slip, which is parameterized for a set of uniformly distributed point sources (subfaults). Ground motion at a given site for either LF and HF bands was obtained separately by summing up time-delayed ground motions from all subfaults for a given rupture velocity and hypocenter location, and then total LF and HF ground motion is added in the time domain. LF ground motion is calculated by using the discrete wave number method [6]. HF ground motion of point sources is calculated using a stochastic method that incorporates a frequency-dependent radiation pattern (see equations 13 to 15 in Pulido and Dalguer (2009) [7]). The idea behind those equations is to incorporate a smooth transition between the theoretical radiation pattern at low frequencies to a complete isotropic pattern at high frequencies due to scattering [5, 7]. The methodology has been extensively tested and validated through modeling of earthquakes in various tectonic regions worldwide [5, 7–9].

Based on the Sladen et al. (2010) source model [1], we simulated BBF strong ground motion at PCN and NNA stations. The source model is characterized by a variable distribution of rise time rupture propagation and stress drop and a constant fault mechanism across the fault plane. For simulation, we simplified the original source model consisting of three fault planes with varying dip representing the geometry of the subducting plate [1] to one single segment where most of the slip was released (**Fig. 2a**). Our fault plane corresponds to the middle segment of the original fault model of Sladen et al. (2010) [1] extended beyond the shallower and deeper edges of that segment with a constant dip of 20°. Our fault model has a strike of 138°, a dip of 20°, and an average rake of 59°. The fault plane was discretized in an array of 16×16 point sources uniformly distributed, with a spacing of 10 km. The shallower row of point sources was located at a depth of 8.9 km. We used the same epicentral location as in Sladen et al. (2010) [1] but slightly modified the hypocentral depth to 35.7 km to be consistent with our source geometry. We used the rupture front propagation results obtained by Sladen et al. (2010) [1] to set the rupture sequence of point sources in our source model (contour lines in **Fig. 2a**). For rise time distribution, we used a modified version of the Sladen et al. (2010) model [1] by applying spatial smoothing around each point source.

4. Estimation of Site Effects

To simulate ground motion in a broad frequency band, it is necessary to take site amplification information into account. Site information was obtained from microtremor measurements near the PCN site as well as in Pisco city using a 3-component velocity sensor with a natural period of 5 s [10]. In this study, we use the horizontal to vertical (HoV) ratio of microtremors at those sites as a proxy for site amplification. Although it is well known that HoV ratios of microtremors do not directly represent site amplification, studies in Japan have shown that HoV ratios can provide first-order approximation to site amplification after appropriate correction depending on the geology of the site [11]. In the case of PCN and Pisco, measured HoV ratios were corrected by a factor of 1.5 appropriate for alluvial sites [11] (**Fig. 3**). In the case of the NNA station, we assume that it is only negligibly affected by site effects because it is located 60 m back in a rock (granite) tunnel.

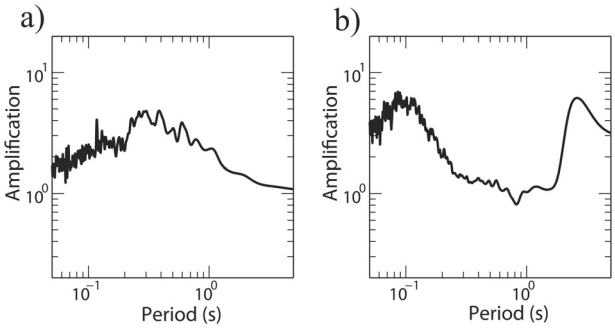

Fig. 3. a) Site amplification at PCN station (−75.6992 longitude, −14.0423 latitude) obtained from HoV ratios of microtremors. b) Same for the Pisco city central square (−76.2028 longitude, −13.7099 latitude).

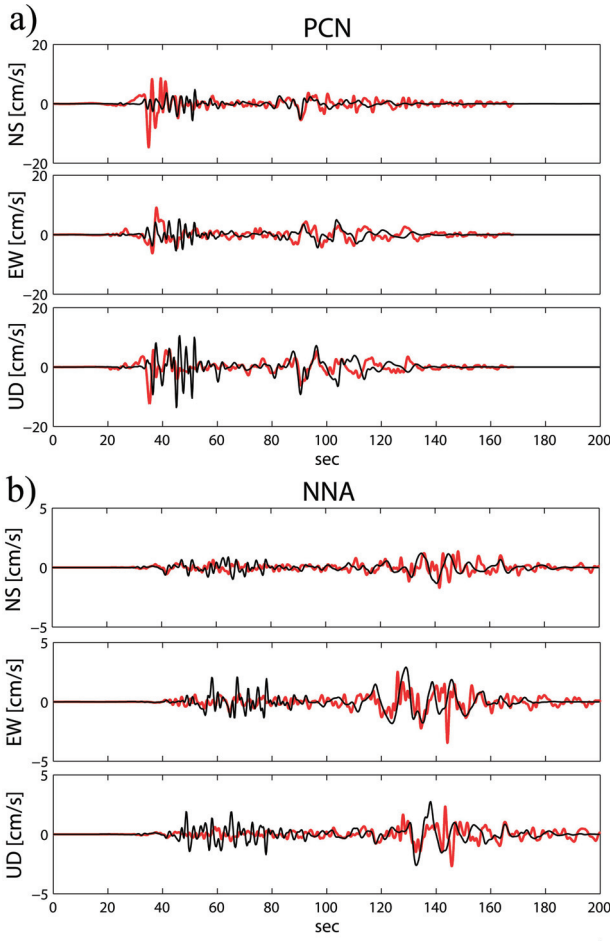

Fig. 4. a) Observed (red) and simulated (black) low frequency (0.05-0.8 Hz) waveforms at PCN. b) Same for NNA.

5. Simulation Results

5.1. LF Waveforms and LF Source Model

In order to check the ability of the aforementioned source model to simulate the observed strong motion, we calculated LF ground motion at stations PCN and NNA. For this purpose, we used a 1D velocity model of the crust appropriate for the region [12]. In **Figs. 4a** and **4b**, we show observed velocities at these stations in red and simulated velocities in black, respectively. Waveforms were band-pass-filtered between 0.05 Hz and 0.8 Hz and rise times were slightly modified to improve fit. We obtained a good agreement between observed and simulated waveforms. These results indicate that the source model can be appropriate to simulate LF waveforms in the near-source region. We subsequently refer to this model as the LF source model.

Table 1. Source parameters for BBF strong motion simulation. Parameters in the lower section of the table fully describe the LF source model.

Parameter	Value
Stress drop distribution	Based on the slip distribution
Duration of ground motion envelopes of point sources (T_w)	From equations 16 and 17 in Pulido and Dalguer, 2009, [7]
Q	$210f^{0.5}$ (f is frequency in Hz) [13]
Average S-wave velocity	3.76 (km/s)
Density	3.1 (T/m^3)
f_{max}	15 Hz
Slip distribution	From [1]
Strike, dip, rake	From [1] (138°, 20°, 59°)
Rupture propagation	From [1]
Rise time distribution	From [1]

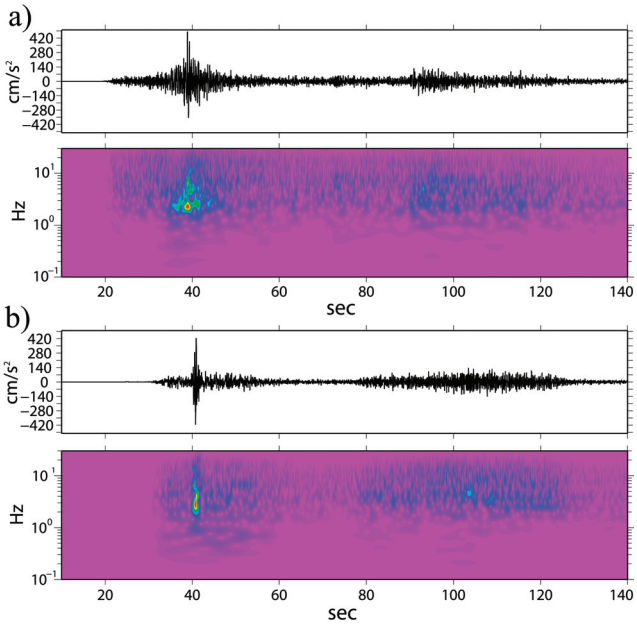

Fig. 5. a) Observed strong motion EW component at PCN (upper panel). S-transform of the EW component at PCN (lower panel). b) Same for simulated EW component at PCN.

5.2. BBF Waveforms and LF Source Model

We then tested the capacity of the LF source model to simulate observed HF ground motion at PCN and NNA stations. The calculation of HF requires the use of additional source parameters such as stress drop distribution (**Table 1**). Stress drop distribution was calculated directly from slip distribution in **Fig. 2a** by using the methodology of Ripperger and Mai (2006) [14]. Using this source model we calculated BBF ground motion at PCN and NNA at a rock site, and for PCN, we convolved it with its site amplification (**Fig. 3a**). Our results show that simulated peak acceleration at PCN (179 cm/s^2) largely underestimates observed peak acceleration (484 cm/s^2). These results indicate that site amplification at PCN did not likely cause the large observed acceleration at this site. In addition, broadband ground motion simulation does not display larger peak acceleration for the first subevent compared to the second subevent, as observed at PCN. Our results show that the LF source model may be appropriate for simulating BBF ground motion at NNA. In the following section, we explore source parameters that may improve HF radiation at PCN.

5.3. BBF Waveforms and BBF Source Model

To understand the time-frequency characteristics of observed ground motion, we calculated the S-transform (a time-frequency localization spectral method [15]) at PCN (**Fig. 5a**). In the lower panel in **Fig. 5a**, we show the S-transform of observed EW component at PCN, which is characterized by a very large localized spectral value near 40 s for a frequency of around 2 Hz. This large spectral energy corresponds to peak acceleration also visible near 40s in the EW record (**Fig. 5a**, upper panel). To locate the possible origin of this peak acceleration within our source model, we calculated the isochrones of PCN across the fault plane (contour lines in **Fig. 2b**). Subfaults located along the isochrone line at 40 s would correspond to possible sources of large acceleration. After exploring the effect of various source parameters on HF ground motions, we found that the large acceleration peak at PCN is adequately reproduced when we assign a stress drop value of 50 MPa to a subfault located 13 km south of the hypocenter (dark red square in **Fig. 2b**, and dashed region in **Fig. 1**). This value is 3 times larger than the stress drop value obtained from slip distribution at this subfault. We also set the duration of the envelope employed to calculate ground motion at PCN to 3 s at this subfault to enhance HF radiation. For remaining subfaults, we use stress drop values from the slip model (**Fig. 2b**) and for other source parameters, we use the same values as for the LF source model. We subsequently refer to this model as the BBF source model. The upper panel in **Fig. 5b** shows that the simulated BBF accelerogram at PCN (EW component) is in very good agreement with the observed record in terms of amplitude and timing of peak acceleration. Time-frequency characteristics of the simulated waveform is also in good agreement with observed ground motion (**Fig. 5b**, lower panel). Note that observed time-frequency characteristics in the PCN record also show additional HF episodes for times around 40 s where the largest acceleration peak was observed, and for frequencies from 2 to 8 Hz (**Fig. 5a**, lower panel). This suggests the possibility that multiple HF events occurred around the hypocenter during the earthquake. In this study, we concentrate mainly on the largest acceleration peak.

We simulated EW, NS and UD components of BBF ground motion at PCN and NNA. In **Figs. 6a** and **6b**, we show observed (in red) and simulated (in blue) acceleration and velocity at PCN and in **Figs. 7a** and **7b**, we show those for waveforms at NNA. Note the good agree-

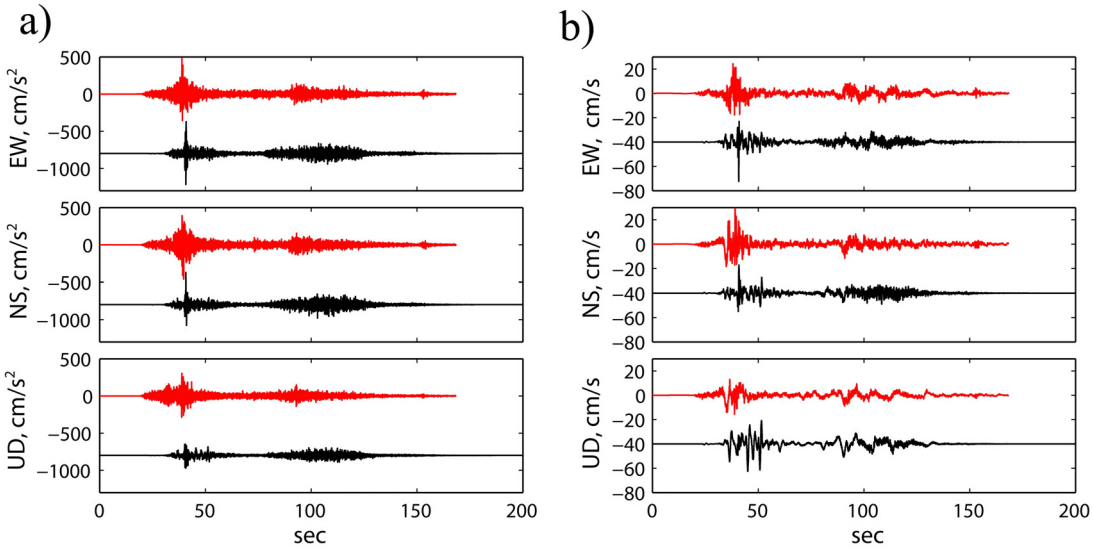

Fig. 6. a) Observed (red) and simulated (black) BBF accelerograms for the EW, NS and UD components at PCN. b) Same for simulated velocities at PCN.

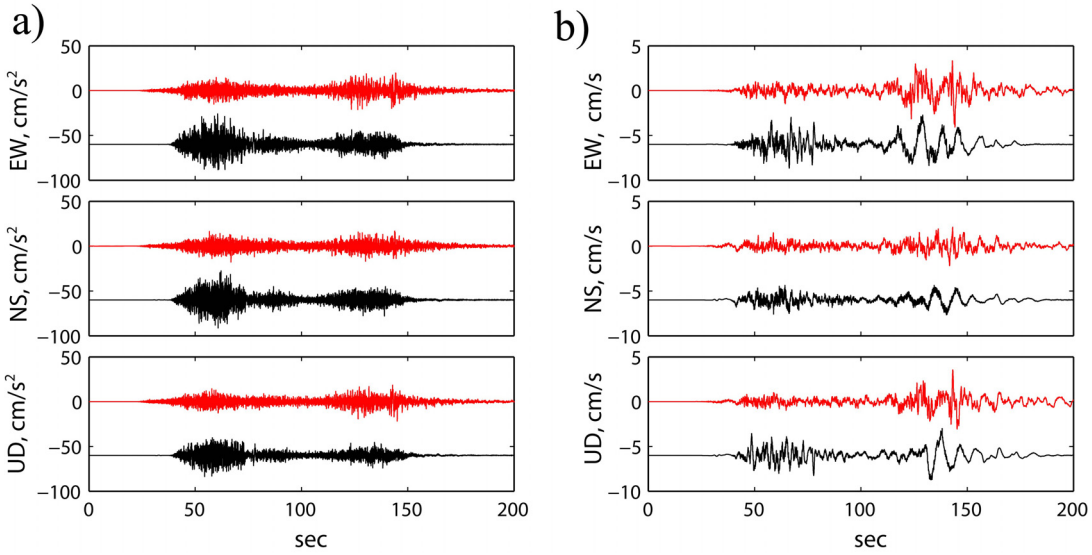

Fig. 7. a) Observed (red) and simulated (black) BBF accelerograms for EW, NS and UD components at NNA. b) Same for station NNA.

ment between observed and simulated waveforms at these stations. We also observed that large simulated peak acceleration within the first subevent at PCN is not visible for the first subevent at NNA, which is in agreement with observation. This feature may be explained by distance-dependent smoothing on ground motion due to scattering that would be stronger for NNA than for PCN and is implemented in our simulation (equations 16 and 17 in Pulido et al. (2009) [7]). There is also good agreement between observed and simulated acceleration and velocity response spectra at PCN (**Figs. 8a** and **8b**, respectively).

5.4. Simulated BBF Waveforms at Pisco City

The city of Pisco, which is located close to the source area, suffered heavy damage during the Pisco earthquake. We simulated BBF waveforms at Pisco central square by incorporating site amplifications from measured microtremors as detailed in Section 4 (**Fig. 3b**). This site exhibits two large peaks of amplification – the first at 0.1 s and the second at 1.5 s. Our simulated waveforms show peak ground acceleration of 701 cm/s^2 and peak velocity of 89 cm/s (**Figs. 9a** and **9b**). These values are more than three times the values obtained for simulation for rock condition at this site and suggest the strong influence of site amplification on strong ground motion (PGA and PGV) in central Pisco. Our simulation also showed two distinct episodes of strong shaking similar to those observed at PCN and NNA. Simulation at Pisco showed that the first episode is characterized by acceleration much larger than the second episode, similar to that for waveforms at PCN, which indicates that the source rupture process of this earthquake may also have made an important contribution to the peak acceleration at Pisco, in addition to site effects. Simulation at Pisco is provided as a first-order approximation to ground motion likely ob-

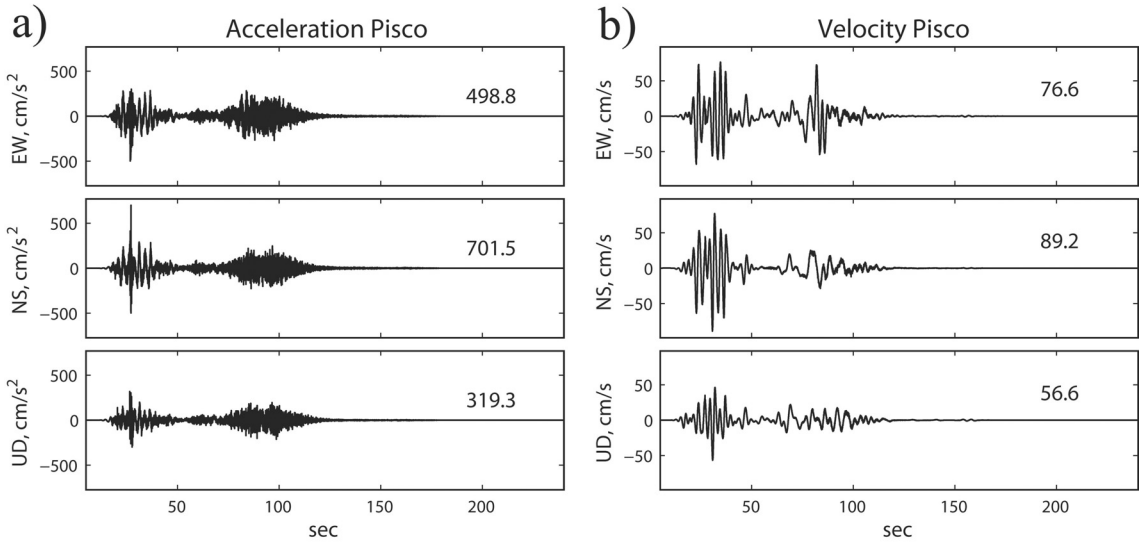

Fig. 9. a) Simulated BBF acceleration waveforms for EW, NS and UD components at Pisco city (central square). b) Same for simulated velocity waveforms at Pisco city (central square).

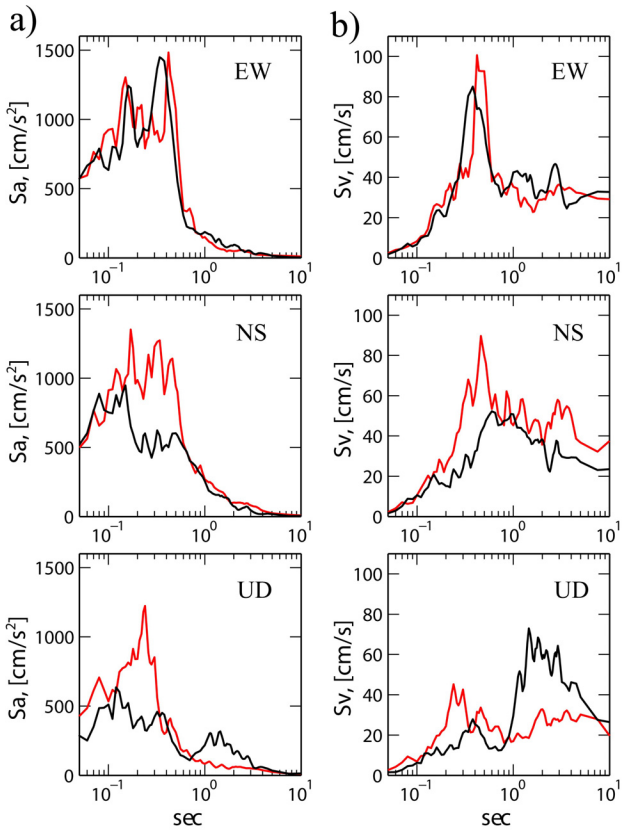

Fig. 8. a) Observed (red) and simulated (black) acceleration response spectra ($h = 0.05$) for EW, NS and UD components at PCN. b) Same for velocity response spectra ($h = 0.05$) at PCN.

served at the city during the earthquake. More detailed analysis regarding site characteristics within Pisco are required, however to study the relationship between ground motion and damage distribution in the city – which is beyond the scope of the present study.

6. Discussion and Conclusions

Our results show that a source model of the Pisco earthquake obtained from long period teleseismic waveforms and InSar data [1] is appropriate in simulating near-source strong motion records filtered in the low frequency range. Our results also show that this model alone cannot reproduce near-source high frequency ground motion.

Our analysis indicates that the large acceleration observed during the first episode of intense shaking at PCN requires the existence of strong high frequency radiation events near the hypocenter. We constructed a source model capable of reproducing this large acceleration at PCN, by locally setting a very large stress drop value at a subfault slightly south of the hypocenter. This may correspond to the rupture of a narrow strong barrier in the vicinity of the hypocenter. Additionally, our observations suggest that multiple high frequency events likely occurred around the hypocenter during the earthquake. Increasing the value of stress drop effectively enhances high frequency radiation. High frequency ground motion may, however, also be radiated from sudden changes in rupture velocity [7]. In order to be able to accurately evaluate these changes, it would be necessary to perform a dynamic model of fault rupture [7]. Dynamic models require detailed knowledge of fault friction parameters and stress fields around the fault, however, and these are generally poorly known.

Our results indicate that the source process of the Pisco earthquake is frequency-dependent. Short-period radiation likely emanated from a region near the hypocentre at 30-40 km depth, whereas the large slip area responsible for long-period radiation was located at a shallower depth, e.g., ∼15 km. The frequency dependence of the source process along the dip has been recently observed in large megathrust earthquakes such as the 2004 Sumatra-Andaman, 2011 Tohoku-oki and 2010 Maule earthquakes, as summarized by Lay et al. (2012) [16]. A

recent study by Sufri at al. (2012) [17] also shows along-the-dip seismic radiation segmentation during the Pisco earthquake. Their study, based on the back-projection of observed teleseismic array data (up to 2 Hz) indicates high frequency energy radiation slightly east of the USGS hypocenter, which is in overall agreement with our findings. Our results indicate, furthermore, that high frequency radiation near the hypocenter was mainly observed from 2 to 10 Hz with a maximum value at 2.5 Hz.

Our results suggest that Pisco city likely experienced very large acceleration and velocity during the earthquake reaching values of about 700 cm/s^2 and 90 cm/s, respectively. Our simulation also indicated that the strong high frequency radiation event near the hypocenter as well as large site amplification around 1.5 s measured at the city contributed much to generating such large values of acceleration and velocity, respectively.

Acknowledgements

This study is being conducted under the JICA/JST project "Enhancement of Earthquake and Tsunami Disaster Mitigation Technology in Peru." Strong motion data at NNA and PCN stations belong to the strong motion network of the Instituto Geofísico del Perú (IGP). We thank Antony Sladen for providing us with his source model of the Pisco earthquake. We thank Hiroshi Arai for providing the results of microtremor measurements near the PCN station and in Pisco city. We also thank the reviewers for checking the paper.

References:

[1] A. Sladen et al., "Source model of the 2007 Mw8.0 Pisco, Peru earthquake: Implications for seismogenic behavior of subduction megathrusts," J. Geophys. Res., Vol.115, B02405, doi:10.1029/2009JB006429, 2010.

[2] M. Motagh, R. Wang, T. R. Walter, R. Bürgmann, E. Fielding, J. Anderssohn, and J. Zschau, "Coseismic slip model of the 2007 August Pisco earthquake (Peru) as constrained by wide swath radar observations," Geophys. J. Int., Vol.174, pp. 842-848, 2008.

[3] M. E. Pritchard and E. J. Fielding, "A study of the 2006 and 2007 earthquake sequence of Pisco, Peru, with InSAR and teleseismic data," Geophys. Res. Lett., Vol.35, L09308, doi:10.1029/2008GL033374, 2008.

[4] T. Lay, C. J. Ammon, A. R. Hutko, and H. Kanamori, "Effects of kinematic constraints on teleseismic finite-source rupture inversions: Great Peruvian earthquakes of 23 June 2011 and 15 August 2007," Bull. Seismol. Soc. Am., Vol.100, pp. 969-994, doi:10.1785/0120090274, 2010.

[5] N. Pulido, and T. Kubo, "Near-Fault Strong Motion Complexity of the 2000 Tottori Earthquake (Japan) from a Broadband Source Asperity Model," Tectonophysics, Vol.390, pp. 177-192, 2004.

[6] M. Bouchon, "A simple method to calculate Green's functions for elastic layered media," Bull. Seismol. Soc. Am., Vol.71, pp. 959-971, 1981.

[7] N. Pulido and L. Dalguer, "Estimation of the high-frequency radiation of the 2000 Tottori (Japan) earthquake based on a dynamic model of fault rupture: Application to the strong ground motion simulation," Bull. Seism. Soc. Am., Vol.99, No.4, pp. 2305-2322, doi: 10.1785/012008016, 2009.

[8] N. Pulido, A. Ojeda, A. Kuvvet, and T. Kubo, "Strong Ground Motion Estimation in the Marmara Sea Region (Turkey) Based on a Scenario Earthquake," Tectonophysics, Vol.391, pp. 357-374, 2004.

[9] M. B. Sorensen, K. Atakan, and N. Pulido, "Simulated strong ground motions for the great M9.3 Sumatra-Andaman earthquake of December 26, 2004," Bull. Seism. Soc. Am., Vol.97, 1A, pp. S139-S151, doi: 10.1785/0120050608, 2007.

[10] H. Arai, personal communication, 2012.

[11] B. Zhao and M. Horike, "Simulation of High-Frequency Strong Vertical Motions using Microtremor Horizontal-to-Vertical Ratios," Bull. Seism. Soc. Am., Vol.93, No.6, pp. 2546-2553, 2003.

[12] S. Hartzell and C. Langer, "Importance of Model Parameterization in Finite Fault Inversions: Application to the 1974 Mw8.0 Peru Earthquake," J. Geophys. Res., Vol.98, No.22, pp. 123-22, p.134, 1993.

[13] M. Raoof and O. Nuttli, "Attenuation of High-Frequency Earthquake Waves in South America," PAGEOPH, Vol.122, pp. 619-644, 1984.

[14] J. Ripperger and P. M. Mai, "Fast computation of static stress changes on 2D faults from final slip distributions," Geophys. Res. Lett., Vol.31, L18610, doi:10.1029/2004GL020594, 2004.

[15] R. G. Stockwell, L. Mansinha, and R. P. Lowe, "Localization of the complex spectrum: the S transform, IEEE Trans. Signal Process," Vol.44, pp. 998-1001, 1996.

[16] T. Lay, H. Kanamori, C. J. Ammon, K. D. Koper, A. R. Hutko, L. Ye, H. Yue, and T. M. Rushing, "Depth-varying rupture properties of subduction zone megathrust faults," J. Geophys. Res., Vol.117, B04311, doi:10.1029/2011JB009133, 2012.

[17] O. Sufri, K. D. Koper, and T. Lay, "Along-dip seismic radiation segmentation during the 2007 Mw 8.0 Pisco," Peru earthquake, Geophys. Res. Lett., Vol.39, L08311, doi:10.1029/2012GL051316, 2012.

Name:
Nelson E. Pulido H.

Affiliation:
Senior Researcher, National Research Institute for Earth Science and Disaster Prevention (NIED)

Address:
3-1, Tennodai, Tsukuba, Ibaraki 305-0006, Japan

Brief Career:

2000- Research Seismologist, Earthquake Disaster Mitigation Research Center (EDM), RIKEN, Japan
2001- Research Seismologist, Earthquake Disaster Mitigation Research Center (EDM), National Research Institute for Earth Science and Disaster Prevention (NIED), Japan
2006- Researcher, National Research Institute for Earth Science and Disaster Prevention (NIED), Japan
2012- Senior Researcher, Earthquake and Volcano Research Unit, National Research Institute for Earth Science and Disaster Prevention (NIED), Japan

Selected Publications:

• N. Pulido, Y. Yagi, H. Kumagai, and N. Nishimura, "Rupture process and coseismic deformations of the February 2010 Maule earthquake," Chile, Earth, Planets and Space, Vol.63, No.8, pp. 955-959, doi:10.5047/eps.2011.04.008, 2011.
• N. Pulido and L. Dalguer, "Estimation of the high-frequency radiation of the 2000 Tottori (Japan) earthquake based on a dynamic model of fault rupture: Application to the strong ground motion simulation," Bull. Seism. Soc. Am., Vol.99, No.4, pp. 2305-2322, doi: 10.1785/012008016, 2009.
• N. Pulido, S. Aoi, and H. Fujiwara, "Rupture process of the 2007 Notohanto Earthquake by using an Isochrones Back-projection Method and K-NET and KiK-net data," Earth Planets and Space, Vol.60, pp. 1035-1040, 2008.
• N. Pulido and T. Kubo, "Near-Fault Strong Motion Complexity of the 2000 Tottori Earthquake (Japan) from a Broadband Source Asperity Model," Tectonophysics, Vol.390, pp. 177-192, 2004.
• N. Pulido and K. Irikura, "Estimation of Dynamic Rupture Parameters from the Radiated Seismic Energy and Apparent Stress," Geophysical Research Letters, Vol.27, pp. 3945-3948, 2000.

Academic Societies & Scientific Organizations:

• American Geophysical Union (AGU)
• Seismological Society of America (SSA)
• Seismological Society of Japan (SSJ)
• Japan Association for Earthquake Engineering (JAEE)

Name:
Hernando Tavera

Affiliation:
Director, Department of Seismology, Geophysical Institute of Peru

Address:
Calle Badajoz # 169 - Mayorazgo IV Etapa - Ate Vitarte, Lima, Peru

Brief Career:
2012 Director, Department of Seismology, Geophysical Institute of Peru
2012 Scientific Researcher, Geophysical Institute of Peru

Selected Publications:
• H. Tavera, "A Report on the 24 August 2011 Mw 7.0 Contamana, Peru, Intermediate-Depth Earthquake," Seismological Research Letters, Vol.83, No.4, doi: 10.1785/0220120005, 2012.
• K. Phillips, R. W. Clayton, P. Davis, H. Tavera, R. Guy, S. Skinner, I. Stubailo, L. Audin, and V. Aguilar, "Structure of the subduction system in southern Peru from seismic array data," J. Geophys. Res., Vol.117, B11306, doi:10.1029/2012JB009540, 2012.
• M. Chlieh, H. Perfettini, H. Tavera, J.-P. Avouac, D. Remy, J.-M. Nocquet, F. Rolandone, F. Bondoux, G. Gabalda, and S. Bonvalot, "Interseismic coupling and seismic potential along the Central Andes subduction zone," J. Geophys. Res., Vol.116, B12405, doi:10.1029/2010JB008166, 2011.
• H. Tavera, I. Bernal, F. Strasser, M. Arango-gavina, J. Alarcon, and J. Bommer, "Ground motions observed during the 15 August 2007 Pisco, Peru, earthquake," Bulletin of Earthquake Engineering, doi:10.1007/s10518-008-9083-4, 2008.

Academic Societies & Scientific Organizations:
• IASPEI, Seismology section (LASC)
• Sociedad Geologica del Peru

Name:
Zenon Aguilar

Affiliation:
Professor, Faculty of Civil Engineering, National University of Engineering

Address:
Av. Túpac Amaru N° 1150, Lima 25, Peru

Brief Career:
1999 Doctoral Student, Kyoto University
2012 Professor, National University of Engineering, Peru
2012 Manager, ZER Geosystem PERU SAC

Selected Publications:
• "Seismic Microzonation of Lima," Japan-Peru Workshop on Earthquake Disaster Mitigation, Japan-Peru Center for Earthquake Engineering and Disaster Mitigation (CISMID), 2005.

Academic Societies & Scientific Organizations:
• American Society of Civil Engineers (ASCE)

Name:
Shoichi Nakai

Affiliation:
Professor, Department of Urban Environment Systems, Chiba University

Address:
1-33 Yayoi-cho, Inage-ku, Chiba 268-8522, Japan

Brief Career:
1984 Dr. Eng., Tokyo Institute of Technology
1978-1997 Shimizu Corporation
1997- Professor, Chiba University

Selected Publications:
• "Estimation of a Deep Shear Wave Velocity Structure of Chiba City Based on Arrays of Seismometers," Journal of JAEE, Vol.12, No.4, pp. 80-93, 2012.

Academic Societies & Scientific Organizations:
• Architectural Institute of Japan (AIJ)
• Japan Association for Earthquake Engineering (JAEE)
• The Japan Geotechnical Society (JGS)

Name:
Fumio Yamazaki

Affiliation:
Professor, Department of Urban Environment Systems, Chiba University

Address:
1-33 Yayoi-cho, Inage-ku, Chiba 263-8522, Japan

Brief Career:
1978 Research Engineer, Shimizu Corporation, Japan
1989 Associate Professor, Institute of Industrial Science, University of Tokyo
2001 Professor, Asian Institute of Technology (AIT), Bangkok, Thailand
2003 Professor, Department of Urban Environment Systems, Chiba University

Selected Publications:
• W. Liu and F. Yamazaki, "Detection of Crustal Movement from TerraSAR-X intensity images for the 2011 Tohoku, Japan Earthquake," Geoscience and Remote Sensing Letters, Vol.10, No.1, pp. 199-203, 2013.
• A. Meslem, F. Yamazaki, and Y. Maruyama, "Accurate evaluation of building damage in the 2003 Boumerdes, Algeria earthquake from QuickBird satellite images," Journal of Earthquake and Tsunami, Vol.5, No.1, pp. 1-18, 2011.

Academic Societies & Scientific Organizations:
• Japan Society of Civil Engineers (JSCE)
• American Society of Civil Engineering (ASCE)
• Seismological Society of America (SSA)
• Earthquake Engineering Research Institute, USA (EERI)